

Supplement Information

Porous metalloporphyrinic nanospheres constructed from metal 5,10,15,20-tetrakis(4'-ethynylphenyl)porphyrin for efficient catalytic degradation of organic dyes

Yongjin Li, Liming Wang, Yong Gao, Weijun Yang*, Yingying Li, Cancheng Guo

College of Chemistry and Chemical Engineering, Hunan University, Changsha 410082, Hunan, China

1. Synthesis of Mn(III) 5,10,15,20-Tetrakis (4'-ethynylphenyl) porphyrin

1.1. Synthesis of 4-[(Tyimethylsilyl)ethynyl]benzaldehyde

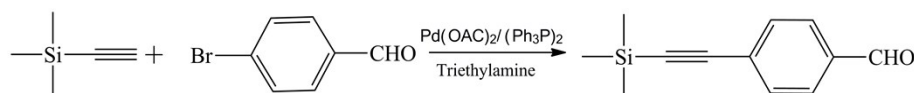


Fig. S1. Synthesis of 4-[(Tyimethylsilyl)ethynyl]benzaldehyde

A mixture of 4-bromobenzaldehyde (740.1 mg, 4 mmol), triphenylphosphine (21.0 mg, 80 μmol), palladium acetate (9.0 mg, 40 μmol) was added into a 100 mL three-necked flask and air was degassed by three cycles of argon gas pump-inflation. Air-removed triethylamine (8 mL) and ethynyltrimethylsilane (471.4 mg, 4.8 mmol) were then injected into the three-necked flask under stirring and refluxed at 76°C for one hour. Finally, the liquid phase was then collected by filtration after being cooled to room temperature and then concentrated to a thick oil which solidified into long needles. The crude product was further purified by silica gel (100-200 mesh) chromatography (petroleum ether / ethyl acetate, 15:1) to give 4-[(Tyimethylsilyl)ethynyl]benzaldehyde (728.1 mg) in 90.11%.

Mass spectrum: (70eV), 202 (15.3, M^+), 187 (100, $\text{M}^+ - \text{CH}_3$);

IR(KBr): 2960 (SiCH), 2825, 2720 (HC=O), 2145 (C \equiv C), 1690 (C=C), 1245 (SiC), 840 cm^{-1} (SiC);

$^1\text{H-NMR}$ (CDCl_3): δ (ppm) 0.21 (s, 9H, SiCH₃), 7.60 (q, 4H, $J=7.0\text{Hz}$, aromatic), 9.85 (s, 1H, CHO);

Anal. Calcd for $\text{C}_{12}\text{H}_{14}\text{OSi}$: C, 71.23; H, 7.33; Si, 13.88. Found: C, 71.31; H, 7.42; Si, 14.01.

1.2. Synthesis of 5,10,15,20-Tetrakis [4'-(trimethylsilyl)ethynylphenyl]porphyrin

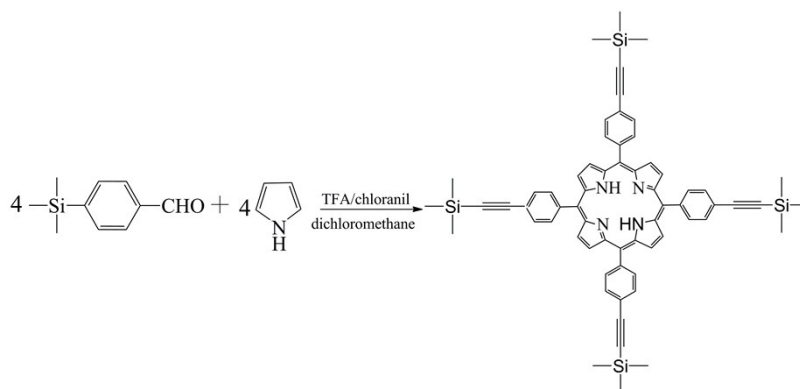


Fig. S2. Synthesis of 5,10,15,20-Tetrakis [4'-(trimethylsilyl)ethynylphenyl]porphyrin

A solid of 4-[(Trimethylsilyl)ethynyl]benzaldehyde (809.3 mg, 4 mmol) was added into a 250 mL three-necked flask and air was degassed by three cycles of argon gas pump-inflation. Air-removed dichloromethane (120 mL) and trifluoroacetic acid (TFA, 0.15 mL) were then injected into the three-necked flask under stirring and added with freshly distilled pyrrole (325.9 mg, 4.8 mmol,) diluted with dichloromethane (30 mL) in 30 min. The reaction mixture was stirred at room temperature for 12h, and chloranil (491.8 mg, 2 mmol) was added into reaction solution continuous reaction for 4h. Finally, the reaction solution was concentrated to a dark solid by rotary evaporation. The dark solid was dissolved in 50 mL of methanol and the precipitate was collected by filtration and washed with methanol until the filtrate being colorless. The crude product was further purified by recrystallization from dichloromethane and methanol (15 mL: 60 mL) three times, dried in vacuum to give [4'-(trimethylsilyl)ethynylphenyl] porphyrin as purple crystalline powder (243.6 mg) in 24.26% yield.

Mass spectrum: (70eV), $m/z=999$ ($M^{+}+1$) 998(M^{+});

$^1\text{H-NMR}$ (CDCl₃): δ 8.81 (b-H, s, 8H_s), 8.14 (o-ArH, d, 8H, 3J=7.80 Hz), 7.86 (m-ArH, d, 8H, 3J=7.80 Hz), 0.372 (Si-CH₃, s, 36H), -2.84 (NH, s, 2H);

IR (KBr): 800 cm^{-1} (C-H), 856.4 cm^{-1} (SiC), 1251.8 cm^{-1} (SiC), 2156.4 cm^{-1} (C \equiv C), 2956.9 cm^{-1} (SiCH₃), 968.3 cm^{-1} (N-H), 3317.5 cm^{-1} (N-H);

UV-Vis (λ ; nm; CHCl₃): 410, 516, 550, 590, 650, 682.

1.3. Synthesis of 5,10,15,20-Tetrakis (4'-ethynylphenyl)porphyrin

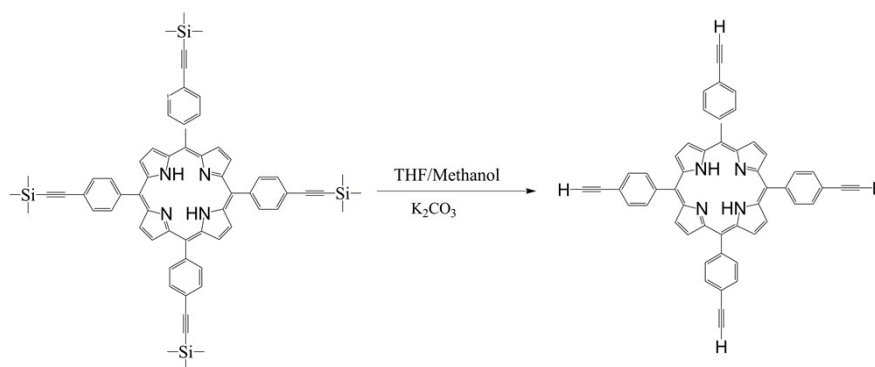


Fig. S3. Synthesis of 5,10,15,20-Tetrakis (4'-ethynylphenyl)porphyrin

A sample of 5,10,15,20-Tetrakis [4'-(trimethylsilyl)ethynylphenyl]porphyrin (100.4 mg, 1mmol) was

dissolved in 20 mL of THF: methanol=3: 1. K_2CO_3 (55.2 mg, 4mmol) was added and the reaction mixture was stirred at room temperature for 4h. The reaction mixture was concentrated to dryness and then the purple solid was redissolved in 20 mL of $CHCl_3$. The organic solution was washed with H_2O and dried $MgSO_4$, filtered, and concentrated to dryness. Column chromatography on silica gel (dichloromethane/hexanes, 1:1) to give 5,10,15,20-tetraksi [4'-ethynylphenyl]porphyrin (640.8 mg) in 90.01%.

Mass spectrum: (70eV), $m/z=711.3 M^+$;

1H -NMR ($CDCl_3$): δ 8.84 (b-H, s, 8H,), 8.17 (o-ArH, d, 8H, 3J=8.40 Hz), 7.90 (m-ArH, d, 8H, 3J=8.40 Hz), 3.33 (CCH, s, 4H), -2.83 (NH, s, 2H);

IR (KBr): $800cm^{-1}$ (s, C-H), $968.3cm^{-1}$ (N-H), $3265 cm^{-1}$ (C \equiv CH), $3317.5cm^{-1}$ (N-H);

UV-Vis ($CHCl_3$): 414, 516, 550, 592, 648.

1.4. Synthesis of Mn(III) 5,10,15,20-Tetraksi (4'-ethynylphenyl) porphyrin

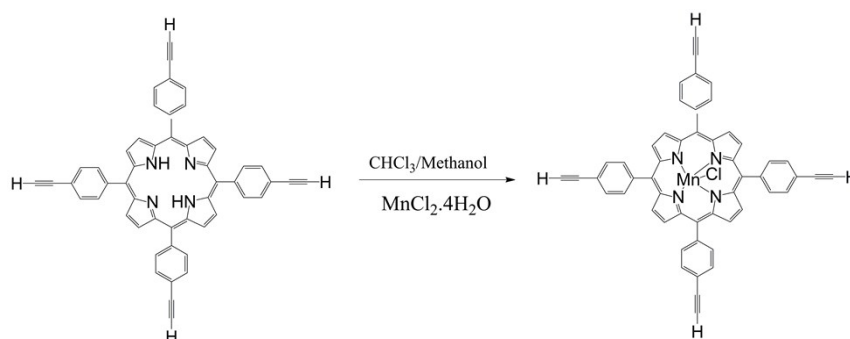


Fig. S4. Synthesis of Mn(III) 5,10,15,20-Tetraksi (4'-ethynylphenyl) porphyrin

A sample of 5,10,15,20-Tetraksi (4'-ethynylphenyl)porphyrin (712.2 mg, 1mmol) was metalated in 50 mL $CHCl_3$ with $MnCl_2 \cdot 4H_2O$ (396.6 mg, 2mmol, 5 mL methanol) over 3h, affording green solid. The crude product was further purified by aluminium oxide (100-200 mesh) chromatography (chloroform /acetone, 10:1) to give Mn(II) 5,10,15,20-Tetraksi (4'-ethynylphenyl) porphyrin (800.5 mg) in 100%.

Mass spectrum: (70eV), $m/z=764.5 (M^+ - Cl)$;

IR (KBr): $1600, 1494cm^{-1}$ (C=C), $1348cm^{-1}$ (C-N), $1007 (\delta Mn-N)$, $808cm^{-1}$ (aromatics), $3293 cm^{-1}$ (C \equiv CH);

UV-Vis (λ ; nm; $CHCl_3$): 480, 582, 622, 682.

2. Methods of characterization

The specific surface areas and pore size distribution were determined by an SA 3100 accelerated surface and porosity analyzer (Beckman Coulter, Inc.) with nitrogen as probing gas at 77 K. The specific surface areas were calculated by the Brunauer-Emmett-Teller (BET) method. The NLDFT theory was utilized to estimate pore size, pore volume and pore distribution. Field emission scanning electron microscopy (FE SEM) was performed by a Hitachi model S4800 microscope. High resolution transmission electron microscopy (HR TEM) was performed by a JEOL model JEM-3010 microscope. FT-IR spectrum was obtained from a Fourier transform infrared spectrometer (IRrestige-21, Shimadzu), and samples were pretreated by being

completely dried and diluted with potassium bromide. UV-Vis absorption spectroscopy was carried out in CHCl_3 on a Cary 100 UV-Vis spectrophotometer (Agilent technologies). The diffuse reflectance spectra of polymer powder samples diluted with BaSO_4 were recorded on a spectrophotometer equipped with integration sphere. The surface wettability of polymers was evaluated through contact angle that was measured by a JC2000D tensiometer and contact angle meter. X-ray photoelectron spectroscopy (XPS) was conducted by a ThermoFisher-VG Scientific ESCALAB 250Xi X-ray photoelectron spectrometer.

Cyclic voltammetry was performed using a CHI660B electrochemical workstation with a three-electrode cell system in which a glassy carbon electrode loading PP-EPMn or PX-EPMn was used as working electrode, a calomel electrode was used as reference electrode, and a Pt wire was used as counter electrode. As to electrode preparation, 6 mg of PP-EPMn or PX-EPMn sample was dispersed in 0.5 mL of solvent mixture containing 11 μL of Nafion (5 wt%) and 0.49 mL of ethanol by sonication for more than 1 h to obtain a stable suspension. Then 10 μL portion of the sample solution was slightly dropped on the surface of the pre-polished glassy carbon electrode. The electrodes were dried overnight at room temperature for measurement. The electrochemical experiments were conducted in 0.1 mol/L $(\text{CH}_3\text{CH}_2)_4\text{NBr}$ CH_2Cl_2 solution, and cyclically scanned at a scan rate of 50 mV/s at room temperature after Ar gas was purged for 10 min.

3. The effects on the catalytic oxidation

3.1. Effects of temperature on the catalytic oxidation

Temperature is an important factor in catalyzed reaction. The molecular motion increases with the temperature elevates, the probability of collisions between the molecular will increase. And the high temperature is beneficial to the reaction with great activation energy so that more activated molecular was to be activated, which increases the reaction rate. Figure S5 shows the influence the degradation of methylene blue at a given reaction temperature (15, 25, 35, 45°C).

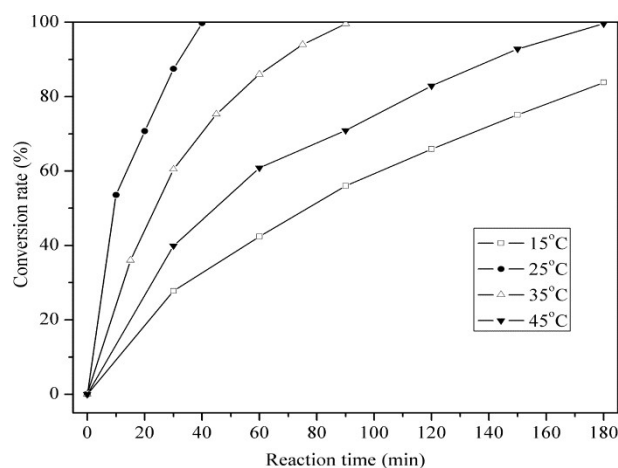


Fig. S5. Effects of temperature on the catalytic oxidation.

According to the Figure S5, the higher the temperature, the rapider the time reach the maximum degradation rate. At 45 °C, it is just 40 min that the degradation rate of methylene blue can reach 99% while it is only 84% degradation rate of methylene blue at 15°C for 3h reaction, what more, we find that the degradation rate of methylene blue could reach 99% only after prolonged degradation time for 4.5h at 15°C. Therefore, raising the temperature of the catalytic system is contributing to the catalytic oxidation of methylene blue, and cut down the time completely degraded.

3.2. Effects of the amount of catalyst on the catalytic oxidation

With PP-EPMn as catalyst degradation methylene blue in the presence of H₂O₂ in neutral condition at room temperature, we had been studied the effect of the amount of catalyst on the reaction by varying the amount of catalyst 2 mg, 3 mg, 4 mg, 5 mg, 6 mg as Figure S6.

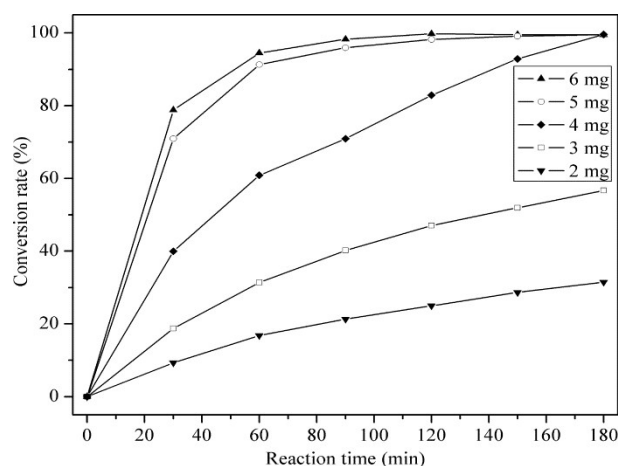


Fig. S6. Effects of the amount of catalyst on the catalytic oxidation.

From Figure S6 can be seen, when the catalyst is 2 mg, the amount of catalyst is insufficient, and the degradation rate is only 35% at 3h. With increasing of the amount of catalyst to 3mg, the reaction time is extended to 8h and the degradation rate can reach 80%. But once the catalyst is greater than 4 mg, the degradation rate increases rapidly, and the time achieved complete degradation is greatly reduced.

3.3. Effects of the concentration of H₂O₂ on the catalytic oxidation at pH=5 and pH=9

The effect of H₂O₂ is importance in the catalytic applications of PP-EPMn. We had been studied the impact of the concentration of H₂O₂ oxidation degradation of methylene blue at pH 5 and 9. The results were shown in Figure S7.

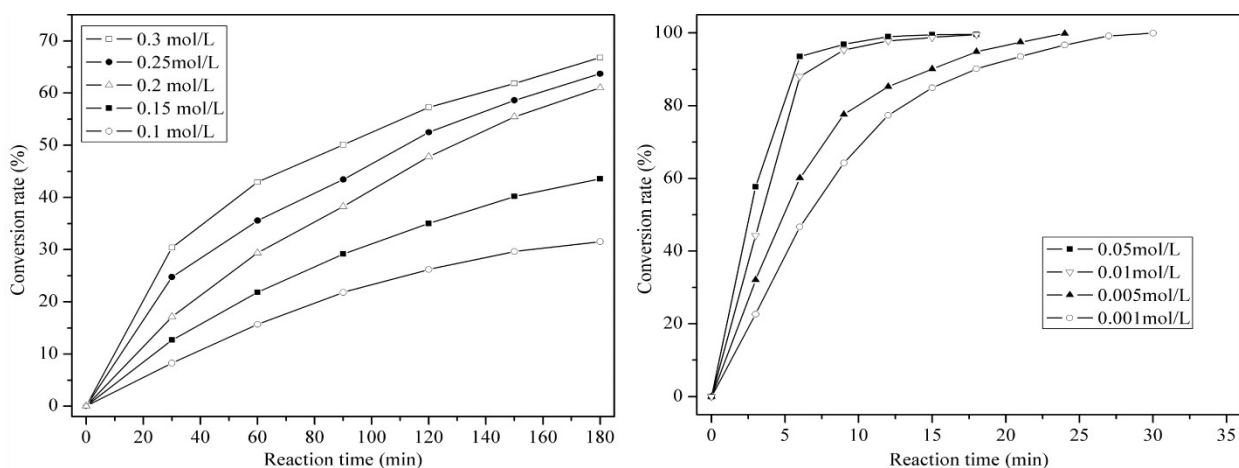


Fig. S7. Effects of the concentration of H_2O_2 on the catalytic oxidation at $\text{pH}=5$ and $\text{pH}=9$.

As shown in Fig. S7. The concentration of methylene blue declined slowly with increasing H_2O_2 at $\text{pH}=5$ and the concentration of H_2O_2 must keep more than 0.2 mol/L , but the concentration of methylene blue declined rapidly with increasing H_2O_2 at $\text{pH}=9$ even the concentration of H_2O_2 is only $1 \times 10^{-3} \text{ mol/L}$. This is mainly because the dissociation of H_2O_2 is difficult at acid pH , and the coordination between $-\text{OOH}$ and Mn^{2+} generated oxomanganese(IV) porphyrin complexes in PP-EPMn is unsuitable for subsequent catalytic oxidation. However, HOO^- dissociated from H_2O_2 in neutral or alkaline conditions is very favorable to coordination with Mn^{2+} in PP-EPMn to generate the oxomanganese(V) porphyrin complexes for expediting the catalytic oxidation [1]. So the PP-EPMn shows good oxidation activity for methylene blue in alkaline condition and the utilization of H_2O_2 is significantly improved.

3.4. Effects of light on the catalytic oxidation

Light is necessary condition to stimulate the catalyst for photocatalytic degradation. So we contrasted the degradation of methylene blue in dark and under light condition, and the results were showed in Figure S8.

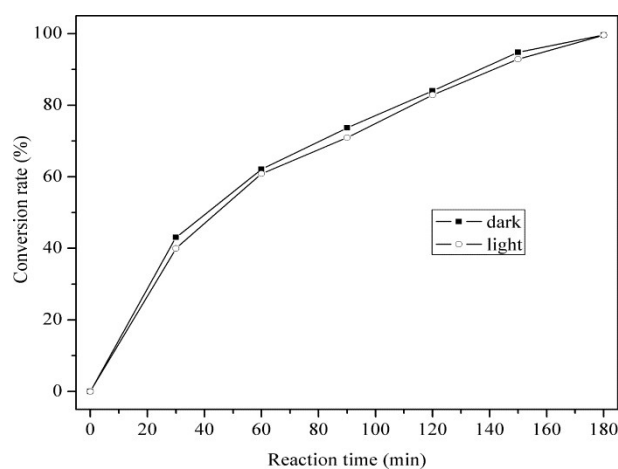


Fig. S8. Effects of light on the catalytic oxidation.

PP-EPMn as catalyst was used for the removal of methylene blue (10 mg/L) in dark and under visible light irradiation (Figure S8). It can be seen from figure S8 that light has little impact on reaction, even in

dark condition the degradation rate is faster than that of under light condition. This shows that the degradation of methylene blue by PP-EPMn is not a photocatalytic reaction but a chemical catalysis reaction, and the presence of light play a role in the degradation of H₂O₂ so that the degradation rate of methylene blue is decreased.

Reference

[1] Wangyang Lu, Nan Li, Wenxing Chen , Yuyuan Yao. Carbon, 2009, 47(14): 3337-3345.